IEEE Access
Multidisciplinary | Rapid Review | Open Access Journal

Received April 1, 2021, accepted April 21, 2021, date of publication May 12, 2021, date of current version June 16, 2021.

Digital Object Identifier 10.1109/ACCESS.2021.3079517

A Ku-Band Compact Disk-Beam Relativistic Klystron Oscillator Operating at Low Guiding Magnetic Field

FANGCHAO DANG, FUXIANG YANG, XINGJUN GE, XINHE WU, AND XIAOPING ZHANG
College of Advanced Interdisciplinary Studies, National University of Defense Technology, Changsha 410073, China

Corresponding author: Fangchao Dang (dangfangchao_nudt@163.com)

This work was supported in part by the National Natural Science Foundation of China under Grant 61901485, and in part by the Natural Science Foundation of Hunan under Grant 2020JJ5662.

ABSTRACT The disk-beam relativistic klystron oscillator (DB-RKO) with the radial-line high frequency structure is one of the attractive high power microwave (HPM) sources due to its specific virtues of weak space-charge effect, high power handling capacity and strong electron collection ability. However, such a device generally exhibits a bulky volume in the radial direction, retarding its actual applications in some compact occasions. Besides, it usually saturates slowly because of the insufficient beam-wave coupling strength. For this purpose, a compact DB-RKO with a rapid saturation process is proposed and physically designed in this paper. By compressing the axial width of the electron beam drift tube suitably, the beam-wave coupling strength is enhanced clearly and the saturation process is accelerated significantly. The whole beam-wave interaction structure is shortened with a radial length of about 5 cm. Besides, in order to increase the device compactness further, an improved magnetic-excited method is presented to enhance the magnetic field in the diode area by introducing a pair of soft-magnets. Furthermore, with the guiding of a low magnetic field of 0.4 T, the compact DB-RKO is experimentally demonstrated to be capable of generating Ku-band HPM radiations with a peak power of 810 MW, a power conversion efficiency of 28%, a center frequency of 14.19 GHz and a pulse duration of about 27 ns. The proposed DB-RKO is promising for the package of the permanent magnets which are preliminarily designed in this paper.

INDEX TERMS High-power microwave, relativistic klystron oscillator, disk electron beam, low guiding magnetic field.

I. INTRODUCTION

High power microwave (HPM) technology has been extensively investigated during the past decades owing to its many potential applications in the civil and military fields [1], [2]. Until now, relativistic vacuum electronic devices continue to be the prominent radiation sources for generating HPMs based on the coherent radiation from an intense relativistic electron beam (IREB) [3]–[14]. Among the multifarious HPM sources, the radial-line microwave devices driven by the disk-shape IREBs are attractive due to their specific merits of weak space-charge effect, high power handling capacity and strong electron collection ability [15]–[17]. In such kind of device, the electron beam is emitted and propagates along the radial direction. The beam density and the space-charge effect are both gradually weakened during its propagation, which is advantageous for the deep modulation of the electron beam and the suppression of the collector erosion caused by the intense electron bombarding. Besides, the resonant cavities are arranged radially and the radio-frequency (RF) field density can be balanced across the output gaps where the RF breakdown easily occurs. So this type of devices is expected to produce microwave radiations in high frequency-bands with high power, high efficiency, low guiding magnetic field and compact size.

Unfortunately, the progress of the disk-beam HPM devices was initially retarded by the electron beam confinement and the slow saturation process [18]–[20]. In some prototype experiments, the output power was much lower than the simulation predictions, which casts doubt on this technical

The associate editor coordinating the review of this manuscript and approving it for publication was Zhilei Yao.

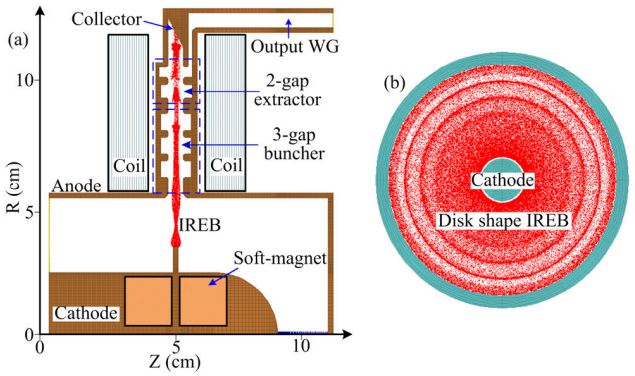

FIGURE 1. Schematic of the ku-band compact DB-RKO: (a) device structure and (b) disk-shape IREB.

scheme. Recently, by improving the electron beam quality and the high frequency interaction structure, we have preliminarily demonstrated the feasibility of this technical scheme with a disk-beam relativistic klystron oscillator (DB-RKO) which was capable of generating Ku-band gigawatt-level microwave radiations in the experiment [21]. However, the previous DB-RKO exhibits an enormous size with a radial dimension larger than 50 cm, which obstructs its actual applications in some lightweight occasions. In this paper, we improve the compactness of this device significantly by designing a higher beam-wave coupling structure and utilizing an improved magnetic-excited method. Besides, the compact DB-RKO is experimentally demonstrated to be capable of generating Ku-band gigawatt-level HPM radiations with a low guiding magnetic field. In addition, the operating feature of the low guiding magnetic field provide possibilities to pack the device with the permanent magnets (PMs) which are preliminarily designed in the end of this paper.

II. DEVICE STRUCTURE

Figure 1 presents the schematic configuration of the Ku-band compact DB-RKO, whose working principle is briefly described as follows. When a high voltage pulse is loaded on the coaxial foiless diode, the disk-shape IREB is emitted from a cusp of the cylindrical cathode based on the explosion emission mechanism. The electron beam propagates radially under the guiding of an external magnetic field, which is supplied by two coils and a pair of soft magnets. The soft-magnets are inserted into the cathode base for compactness. The beam-wave interaction structure mainly consists of a three-gap buncher, a double-gap extractor and several radial-line drift tubes. In the three-gap buncher, the disk electron beam is highly modulated by the TM_{01} mode, which is a standing wave and established based on the transit-time effect. Then, the beam modulation current gets maximal after a short drift. The axial width of the radial-line drift tubes is designed as 6 mm with a cut-off frequency of 25 GHz for the TM_{01} mode. Whereafter, a double-gap extractor is followed closely and plays a role in converting the microwave energy from the well-bunched IREB. Finally, the extracted HPMs are radiated through a coaxial waveguide with TEM mode.

III. COMPACT DESIGN AND PHYSCIAL ANALYSIS

Because of the radial expansion of the disk electron beam, the beam-wave interacting impedance of the DB-RKO is inversely proportional to the beam radius approximately, a feature requires special considerations. It makes the device saturate slowly compared with the popular annular beam HPM devices. In order to accelerate the saturation process, the device was generally designed to operate at a low diode impedance in initial studies [22]–[25]. However, the low diode impedance requires the anode-cathode distance must be minimized much closer, which may lead to the closure of the diode caused by the plasma expansion especially in the long-pulse condition [26]. An alternative solution for this issue is to add the resonant cavities to improve the beam-wave coupling strength. Yet, the whole device would become cumbersome to some extent, limiting its practical applications in some compact occasions. In this section, the design principles and the physical analyses of a compact DB-RKO are illustrated in detail.

A. DESIGN OF BEAM-WAVE INTERACTION STRUCTURE

When the electron beam passes through the buncher of the DB-RKO, an eigen-mode is excited inside the buncher based on the transit-time effect and modulates the electron beam in turn. A small-signal theory by calculating the beam-coupling conductance ratio is generally used to analyze the mode selection and the start-oscillation process [27], [28]. For a three-gap buncher, the $2\pi/3$ mode is usually chosen as the working mode because its conductance ratio stays negative around the diode voltage of hundreds of kilovolts. Figure 2(a) shows a typical structure of a radial-line three-gap buncher and its electric field distribution of the $2\pi/3$ mode. L_1 and L_2 are the axial widths of the resonators and the drift tubes, respectively. The radial electric field profile of the $2\pi/3$ mode can be described as $E_r \sim E_0 f(r) \exp(j\omega t)$, where E_0 is the electric field amplitude, $f(r)$ is the normalized field distribution and ω denotes the angular frequency of the RF field. When the diode voltage is defined, the electron velocity υ_e would be fixed. The gap coupling coefficient M can be calculated by

$$M = \frac{\int_{r_1}^{r_2} f(r) e^{j\beta_e r} dr}{\int_{r_1}^{r_2} |f(r)|\, dr}, \tag{1}$$

where $\beta_e = \omega/\upsilon_e$ is the electron phase-shift coefficient. Substituting (1) into

$$G_e/G_0 = -\frac{1}{4}\beta_e \frac{\partial M^2}{\partial \beta_e}, \tag{2}$$

one can obtain the beam-loading conductance ratio.

Keeping $L_1 = 12$ mm unchanged, the conductance ratios are plotted in Fig. 2(b) under the cases of $L_2 = 6$ mm and $L_2 = 7$ mm. The conductance ratios remain negative around the beam voltage of 400 kV, which indicates the $2\pi/3$ mode

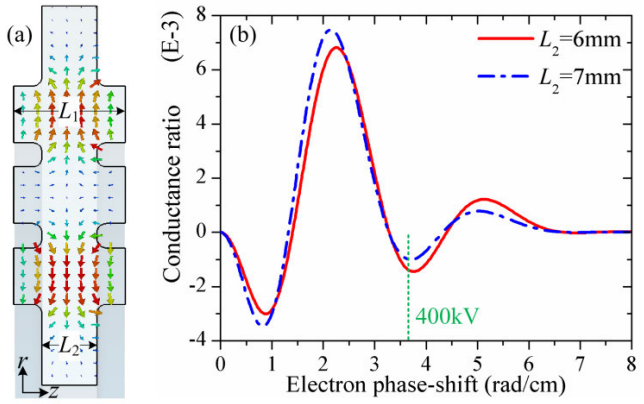

FIGURE 2. The three-gap buncher: (a) electric field distribution of $2\pi/3$ mode and (b) normalized electron beam-loading conductance ratio.

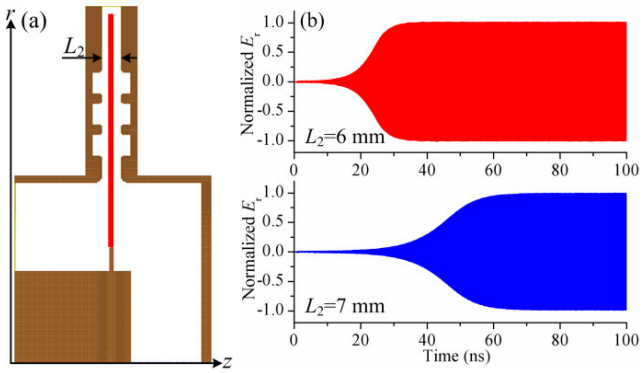

FIGURE 3. Simulations of the three-gap buncher: (a) PIC model and (b) waveforms of the RF electric field.

can be excited during the transition of an intense electron beam. Meanwhile, it can be also found that the conductance ratio amplitude in the case of $L_2 = 6$ mm is much larger than that in the case of $L_2 = 7$ mm around the diode voltage of 400 kV. It means that when $L_2 = 6$ mm, the electron beam will deliver more energy to the RF fields after the electron beam transits through the buncher one time and the RF fields may get saturated with fewer electron transition periods. It should be mentioned that the L_2 is selected as 7 mm in the previous designs of the Ku-band DB-RKO [20]–[22]. The reduction of the saturation duration is mainly realized by decreasing the diode impedance and adding the beam-wave interacting resonant cavities.

In order to validate the above assumption, we build the physical model of the three-gap buncher of the DB-RKO (as shown in Fig. 3(a)) in a particle-in-cell (PIC) simulation code CHIPIC which has been widely verified in the design of HPM devices [29]. The diode voltage and beam current are configured as 400 kV and 6 kA respectively with a rise-time of 2 ns. A guiding magnetic field of 0.4 T is loaded to confine the disk IREB. The waveforms of the gap electric fields of the two cases are displayed in Fig. 3(b), It can be seen that the RF field gets saturation at $t \approx 38$ ns in the case of $L_2 = 6$ mm while the saturation duration is prolonged to $t \approx 65$ ns in the case of $L_2 = 7$ mm. It indicates that the saturation process

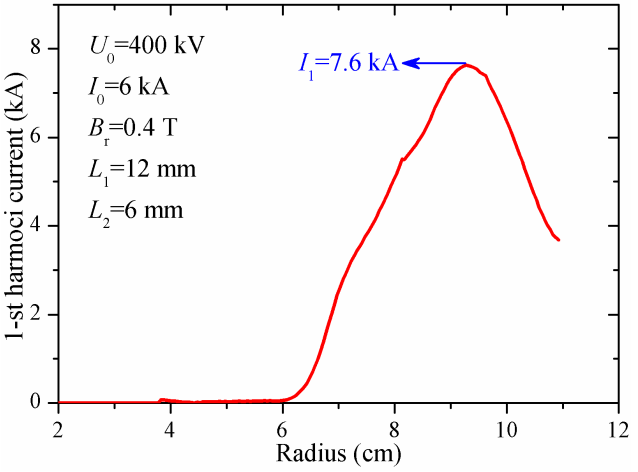

FIGURE 4. Fundamental harmonic modulation current of the three-gap buncher.

can be accelerated significantly by decreasing the axial width of the radial-line drift tube befittingly. In fact, the drift tube has the key function of cutting off the TM_{01} operation modes in the resonant cavities. When the L_2 is decreased from 7 mm to 6 mm, the TM_{01} working mode will be attenuated more quickly in the drift tube. Thus, the RF fields will be more concentrated in the resonant cavities and the beam-wave coupling will be strengthened. The enhanced beam-wave coupling is very advantageous to the start-oscillation and the power conversion for the DB-RKO. Figure 4 shows the fundamental harmonic modulation current distribution of the three-gap buncher. It can be found that the fundamental harmonic modulation current I_1 grows gradually in the buncher and reaches the peak of about 7.6 kA, which denotes a bunching depth I_1/I_0 of 126% where I_0 is the averaged beam current.

After the electron beam is fully modulated by the three-gap buncher, an extractor is followed to extract the microwave energy from the bunched electron beam as much as possible. Generally, the output power P_{out} of a klystron can be expressed by

$$P_{\text{out}} = \frac{1}{2} I_1 \cdot (MV_1) \cos \psi, \tag{3}$$

where M is the gap coupling coefficient of the extractor, the V_1 is the gap voltage across the extractor, and Ψ denotes the phase difference between the space-charge wave and the RF fields. When the fundamental harmonic modulation current I_1 gets maximal, one should enhance the gap coupling coefficient M suitably to improve the output power. In the previous study, a three-gap extractor has been testified to have a capacity of extracting the microwave power with an efficiency of about 35%. In this design, in order to compress the radial dimension of the device, we are inclined to utilize a double-gap extractor to achieve an equal power conversion efficiency. Nevertheless, if the gap number of the extractor is decreased, the output power would be reduced accordingly due to the absence of the additional decelerating

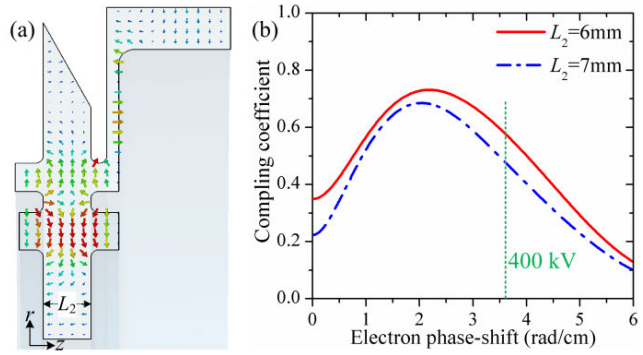

FIGURE 5. The double-gap extractor: (a) electric field distribution of π mode and (b) gap coupling coefficient.

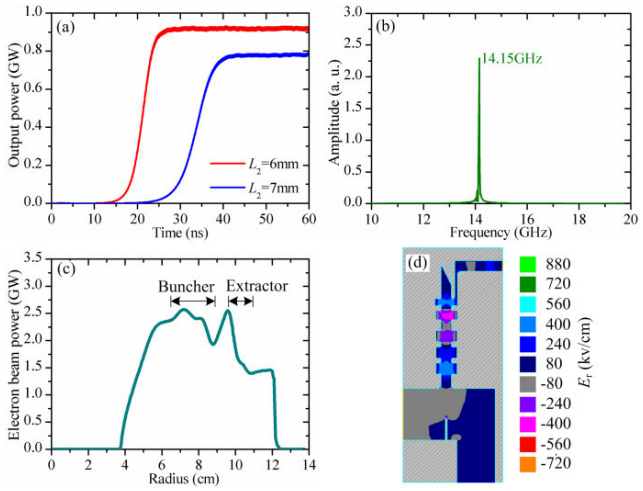

FIGURE 6. Typical simulation results: (a) output power, (b) microwave frequency spectrum, (c) positive power flow of the electron beam and (d) radial electric field distribution.

voltage across the last gap. Therefore, other measures must be exploited to strengthen the beam-wave interaction in the extractor. Figure 5(a) displays the double-gap extractor and the electric field distribution of the π mode. According to (1), one can attain the gap coupling coefficient of the double-gap extractor shown in Fig. 5(b). It is clear that the gap coupling coefficient has a considerable increasement when the L_2 is changed from 7 mm to 6 mm. The higher gap coupling coefficient will help the output cavity to extract more energy from the bunched electron beam. It inspires us to employ a narrower drift tube for the design of the double-gap extractor.

Based on the above physical analysis of the beam-wave interactions of the buncher and the extractor, we select the axial width of the radial-line drift tube as 6 mm to accelerate the saturation process and to improve the beam-wave coupling strength of the presented DB-RKO. The whole device structure is the same as that shown in Fig. 1. The electron beam parameters and the magnetic field strength remain the same as above. The structure parameters are optimized carefully in the PIC simulation. Typical simulation results are illustrated in Fig. 6. The output microwave gets the peak at $t \approx 27$ ns (see Fig. 6(a)). It is found the whole oscillator saturates more quickly compared with PIC model of the single three-gap buncher. That is because the electron beam is modulated further in the extractor after passing through the buncher in the start-oscillation stage. The RF energy stored in the extractor partially couples into the buncher and benefits the growing of the $2\pi/3$ mode. The phase of the coupled RF energy into the buncher can be controlled by adjusting the length of the drift tube between the buncher and extractor. The output power of the DB-RKO reaches 920 MW, indicating a beam-wave conversion efficiency of about 38%. As shown in Fig. 6(b), the main frequency of the output microwave is 14.15 GHz. The case of $L_2 = 7$ mm is also optimized and compared in Fig. 6(a). The saturation duration is prolonged to be $t \approx 42$ ns. Besides, the output power is decreased less than 800 MW. Figure 6(c) displays the positive power flow of the electron beam. It is found the electron beam is continuously decelerated during the two gaps of the extractor. Meanwhile, it is noted that the first gap shares the most beam-to-wave power conversion. That is because the microwave output channel is directly coupled with the second gap, which has a lower circuit impedance compared with the first gap. This feature agrees with the field distribution of the cold cavity in Fig. 5(a). After saturation, the radial electric field is distributed in Fig. 6(d). As is expected, the $2\pi/3$ mode and the π mode are excited in the three-gap buncher and in the double-gap extractor, respectively. Moreover, the length of the beam-wave interaction structure remains only about 5 cm, which is clearly shortened by comparison with the previous DB-RKOs [18]–[20].

B. IMPROVEMENT OF MAGNETIC-EXCITED METHOD

Another problem limiting the compactness of the DB-RKO is the conducting magnetic field, which is mainly excited by two groups of coils with the same structure and current amplitude but the opposite current directions [22], [30]. However, the previous configuration is not suitable for the miniaturized design of the DB-RKO. In that case, the radial magnetic field strength B_r is decreasing quickly when the radius is lower than the inner radius R_c of the solenoids (see Fig. 7). Thus, the diode has to be partially inserted into the narrow space between the two coils and its radial demission generally satisfies $R_a \approx 2R_c$, where R_a denotes the radius of the diode anode. Besides, because the coaxial part of the diode is structurally encircled by the magnetic coils, the R_c cannot be designed too small due to the risk of the electrical breakdown between the cathode-anode gap of the diode. Therefore, the radial dimension of the DB-RKO is generally oversized.

In order to address this problem, we introduce a pair of soft-magnets ($\mu_r \gg 1$) to improve the distribution of the magnetic field. This pair of soft-magnets is foisted into the cathode base and is configured symmetrically respecting to the electron beam channel (see Fig. 1). By Computer Simulation Technology (CST) electromagnetic studio, the magnetic field is calculated and illustrated in Fig. 7. It can be seen that the magnetic field is significantly strengthened in the range

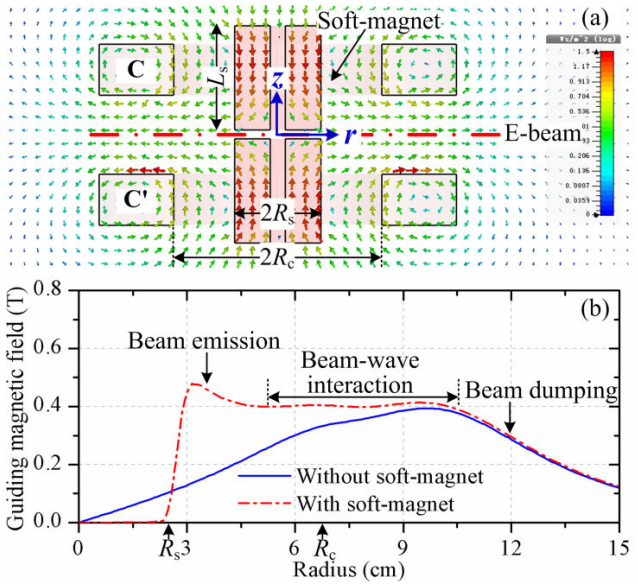

FIGURE 7. Improved magnetic-excited method: (a) structure and the magnetic field distribution and (b) radial magnetic field distribution along the electron beam channel.

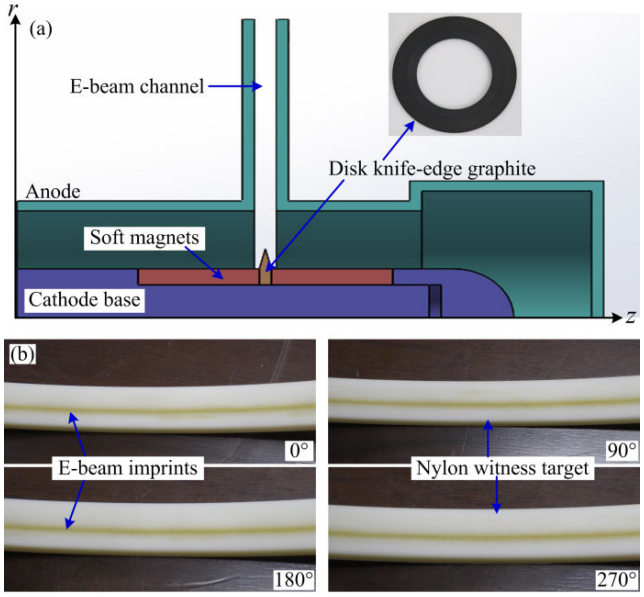

FIGURE 8. Generation of the disk IREB: (a) configuration of the diode and (b) electron beam imprint on the ring-shaped nylon witness target.

$R_s < r < R_c$ compared with the case without the soft-magnets. In fact, owing to their ultrahigh relative permeability $\mu_r \gg 1$, the soft-magnets would dramatically pull the nearby magnetic field lines surrounding them. Such peculiarity of attraction will largely strengthen the axial magnetic field B_z inside the soft-magnets. The enhanced two axial magnetic fields are opposite in the direction and will be extruded with each other at the electron beam channel, which yields an additional radial component magnifying the local conducting magnetic field. Assigning the length and the radius of the soft-magnet $L_s = 7$ cm and $R_s = 2.8$ cm respectively, the radial magnetic field strength at $r \approx 3.6$ cm is largely increased to 0.45 T from 0.15 T. By this method, the diode dimension can be remarkably compressed. The radii of the electron emission and anode wall in this design are reduced to 5.5 cm and 3.6 cm respectively, which are in obvious contrast with the radii of 12 cm and 9 cm in the previous DB-RKO [22]. Besides, the conducting magnetic field appears a uniform distribution with an amplitude of about 0.4 T at the beam-wave interaction area, which lays the foundation of the efficient beam-wave power conversion.

IV. EXPERIMENTAL RESULTS

The compact Ku-band DB-RKO is operated on a SINUS-type electron beam accelerator with a full width at half maximum (FWHM) pulse duration of about 55 ns. The disk electron beam is emitted from a knife-edge disk-shape cathode made of the graphite material (shown in Fig. 8(a)). The graphite cathode is located along the centerline of the radial-line drift tube and clamped between the two soft magnets. The right-end of the cathode base is chamfered to avoid the over-strong electric field. The magnetic coils are powered by a group of charged capacitors. The diode voltage and the diode current are monitored by a capacitance voltage divider and a Rogowski coil surrounding the cathode stick, respectively. The DB-RKO is placed inside a vacuum chamber pumped down by a turbo pump to be $< 1 \times 10^{-2}$ Pa.

Before the HPM generation experiment, the disk IREB is firstly diagnosed by a ring-shaped nylon witness target with an axial width of 10 mm. The witness target is inserted into the first gap of the double-gap extractor. When an IREB attacks the nylon witness target, a yellow imprint would be stigmatized, which helps us to estimate the quality of the electron beam. Under the guiding of a magnetic field of 0.4 T, Figure 8(b) shows the electron beam imprint after one shot. It can be seen that the electron beam imprint exhibits a basically uniform distribution along the azimuthal direction. It indicates the electron beam is emitted uniformly by the knife-edge graphite cathode. Besides, the improved magnetic-excited method is experimentally testified to be capable of guiding the disk IREB well. The axial width of the electron beam imprint is measured less than 2 mm, which means the vast majority of the electron beam can be able to pass through the beam-wave interaction structure almost without loss.

Typical experimental results are illustrated in Fig. 9. When a high voltage pulse of 420 kV is loaded to the DB-RKO, the emitted diode current is monitored to be 6.8 kA. The radiated HPM is measured by the crystal detectors located 6.5 m far away from the launching antenna. The microwave components of the whole measurement circuit are all calibrated carefully by a high precision vector network analyzer (VNA). In order to validate the improvement of decreasing the saturation duration, the simulation microwave waveform under the condition of the experimental waveforms of the diode voltage and the diode current is also plotted in the Fig. 9(a). It can be seen that the generated microwave has

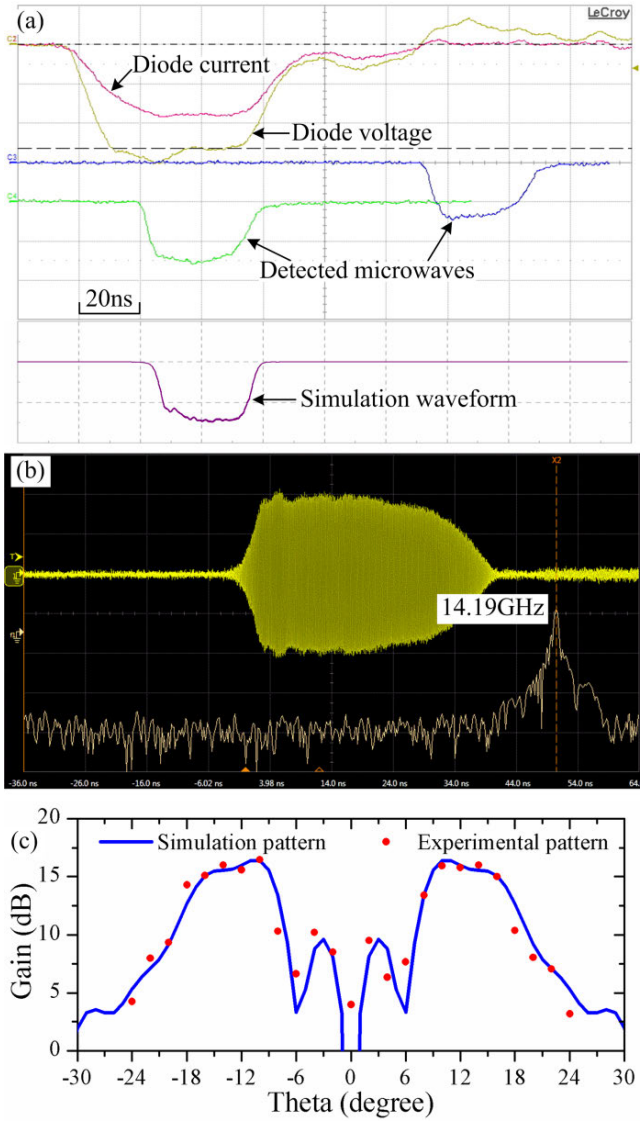

FIGURE 9. Experimental results of the ku-band compact DB-RKO: (a) waveforms of the detected microwaves, (b) its frequency spectrum and (c) far-field power density distribution.

a pulse duration of about 27 ns, which is very close to that of the simulation waveform. The microwave frequency is 14.19 GHz. By integrating the far-field power densities over the azimuthal angle range $\theta \sim [-24°, 24°]$, the peak power is calculated to be 810±30 MW, indicating a power conversion efficiency of about 28%.

V. DESIGN OF PERMANENT MAGNETS

Owing to the weakened space-charge effect, the DB-RKO has been experimentally demonstrated to be capable of producing the gigawatt-level HPMs with a low magnetic field of 0.4 T. Besides, the device has a short axial width ($\sim$ the wavelength λ), which may provide potentials to be packaged by the permanent magnets (PMs). Because of the absence of power supply for the magnetic coils, the permanent magnet packaged HPM devices will be much more efficient and would have a broader application prospect. For this purpose,

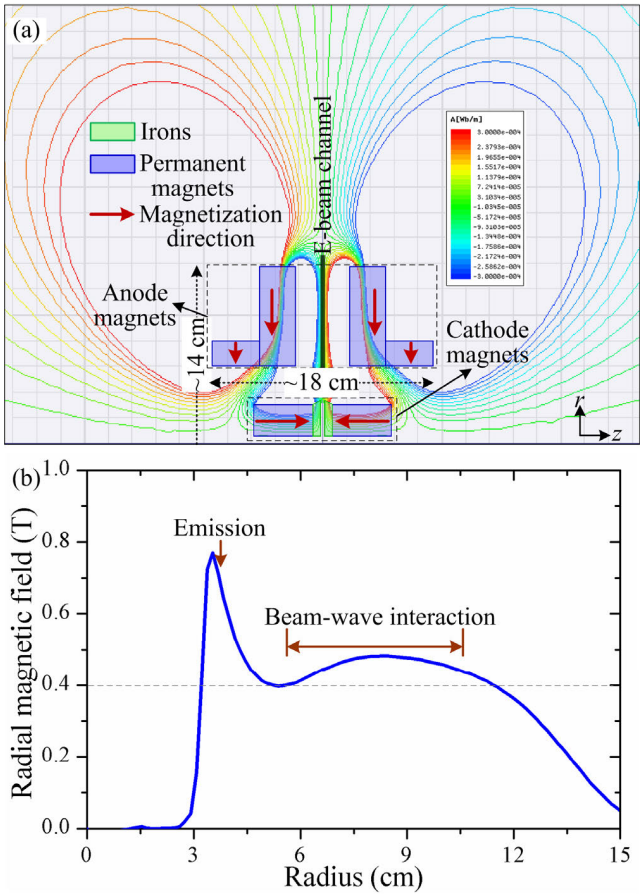

FIGURE 10. Permanent magnets: (a) structure and field distribution, and (b) radial magnetic field variation along the electron beam channel.

a PM system is designed and illustrated in Fig. 10(a). The whole PM system is composed of two parts which are located symmetrically along the electron beam channel. Each part consists of an anode PM, a cathode PM and a soft magnet. The anode PM exhibits an "L"-shape and is magnetized along the radial inward direction. The cathode PM appears a cylindrical structure and is magnetized along the axial direction. The soft magnet is adsorbed on the one side of the cylindrical cathode PM. It should be mentioned that the two cathode PM must be magnetized along the opposite directions to produce a radial magnetic field component.

In the design, the PM materials are selected as the NdFeB N50 which is widely applied in the industry field and owns a remanence of 1.4 T and an intrinsic coercive force of 1 MA/m. Figure 10(b) shows the radial magnetic field variation along the electron beam channel. It is can be seen that the magnetic field strength is larger than 0.4 T in the whole beam-wave interaction region, which is sufficient for the confinement of the above disk IREB. The difference compared with the distribution curve of Fig. 7(b) is that the magnetic field presents some fluctuations in the beam-wave interaction region. Even so, it is also able to constrain the disk IREB well almost without any axial deflection. That is because the there is always no axial magnetic field component at the electron beam channel

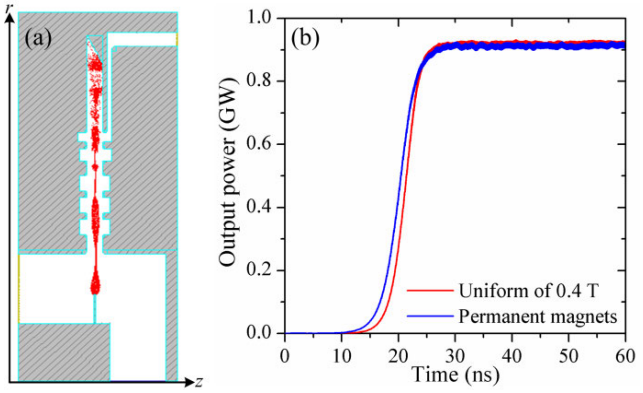

FIGURE 11. Simulation results of the PM packaged DB-RKO: (a) electron beam trajectory and (b) output power.

due to the symmetrical configuration of the two PM parts with respect to the beam channel. Such characteristic is very different from the situation in the axial HPM source driven by an annular IREB. Figure 11 displays the simulation results of the electron beam trajectory and the output power when the designed PM magnetic field is loaded into the Ku-band DB-RKO. It is found that disk electron beam is focused well around the centerline of the high frequency structure. In addition, the output power shows little change compared with the case of the uniform magnetic field, which preliminarily demonstrates the feasibility of the designed PM system.

VI. CONCLUSION

The application of the DB-RKO is limited by its bulky volume and the slow saturation duration. In order to address this issue, a Ku-band compact DB-RKO is proposed and physically designed in this paper. The beam-wave coupling coefficients with different axial widths of the electron beam drift tube are analyzed and compared. It is found that when the axial width is reduced from 7 mm to 6 mm, the beam-wave coupling strength is enhanced and the saturation process is accelerated significantly. The whole beam-wave interaction structure appears a short radial length of about 5 cm. Besides, by introducing a pair of soft-magnets inserted into the cathode base, an improved magnetic-excited method is presented to enhance the magnetic field in the diode area. In this way, the DB-RKO will be designed much more compact compared with the previous cases. In the experiment, the improved magnetic-excited method is validated to confine the disk IREB within an axial width of less than 2 mm under the guiding magnetic field of 0.4 T. Moreover, the compact DB-RKO is demonstrated to be capable of generating Ku-band HPM radiations with a peak power of 810 MW, a power conversion efficiency of 28% and a pulse duration of about 27 ns. Meanwhile, the proposed compact DB-RKO is very promising for the permanent magnet packaging, which may provide an alternative solution for the miniaturized and low energy-cost HPM devices.

REFERENCES

[1] J. Benford, J. A. Swegle, and E. Schamiloglu, *High Power Microwaves*, 3rd ed. Boca Raton, FL, USA: CRC Press, 2016.
[2] S. D. Korovin, V. V. Rostov, S. D. Polevin, I. V. Pegel, E. Schamiloglu, M. I. Fuks, and R. J. Barker, "Pulsed power-driven high-power microwave sources," *Proc. IEEE*, vol. 92, no. 7, pp. 1082–1095, Jul. 2004, doi: 10.1109/JPROC.2004.829020.
[3] A. I. Klimov, I. K. Kurkan, S. D. Polevin, V. V. Rostov, and E. M. Tot'meninov, "A multigigawatt *X*-band relativistic backward wave oscillator with a modulating resonant reflector," *Tech. Phys. Lett.*, vol. 34, no. 3, pp. 235–237, Mar. 2008, doi: 10.1134/S1063785008030176.
[4] N. S. Ginzburg, A. W. Cross, A. A. Golovanov, G. A. Mesyats, M. S. Pedos, A. D. R. Phelps, I. V. Romanchenko, V. V. Rostov, S. N. Rukin, K. A. Sharypov, V. G. Shpak, S. A. Shunailov, M. R. Ulmaskulov, M. I. Yalandin, and I. V. Zotova, "Generation of electromagnetic fields of extremely high intensity by coherent summation of Cherenkov superradiance pulses," *Phys. Rev. Lett.*, vol. 115, no. 11, Sep. 2015, Art. no. 114802, doi: 10.1103/PhysRevLett.115.114802.
[5] Y. Cao, Z. Song, P. Wu, Z. Fan, Y. Zhang, Y. Teng, and J. Sun, "Effective suppression of pulse shortening in a relativistic backward wave oscillator," *Phys. Plasmas*, vol. 24, no. 3, Mar. 2017, Art. no. 033109, doi: 10.1063/1.4977811.
[6] M. I. Fuks and E. Schamiloglu, "Application of a magnetic mirror to increase total efficiency in relativistic magnetrons," *Phys. Rev. Lett.*, vol. 122, no. 22, Jun. 2019, Art. no. 224801, doi: 10.1103/PhysRevLett.122.224801.
[7] X.-J. Ge, P. Zhang, C.-Y. Zhao, Z.-C. Luo, S.-Y. Chen, H.-W. Yang, and J. Zhang, "A high-efficiency L-band coaxial three-period relativistic Cherenkov oscillator," *Sci. Rep.*, vol. 9, no. 1, p. 12244, Aug. 2019, doi: 10.1038/s41598-019-47496-8.
[8] R. Xiao, Y. Deng, C. Chen, Y. Shi, and J. Sun, "Generation of powerful microwave pulses by channel power summation of two X-band phase-locked relativistic backward wave oscillators," *Phys. Plasmas*, vol. 25, no. 3, Mar. 2018, Art. no. 033109, doi: 10.1063/1.5022808.
[9] Y. Wu, Z. H. Li, H. Q. Xie, Z. Xu, and Q. S. Ma, "An S-band high gain relativistic klystron amplifier with high phase stability," *Phys. Plasmas*, vol. 21, no. 11, Nov. 2014, Art. no. 113107, doi: 10.1063/1.4901811.
[10] Z. B. Liu, H. Huang, X. Jin, S. F. Li, T. F. Wang, and X. H. Fang, "Investigation of an *X*-band long pulse high-power high-gain coaxial multibeam relativistic klystron amplifier," *IEEE Trans. Electron Devices*, vol. 66, no. 1, pp. 722–728, Jan. 2019, doi: 10.1109/TED.2018.2879193.
[11] H. Huang, Z. Chen, H. He, H. Yuan, Z. Liu, and L. Lei, "Investigation on pulse-shortening of S-band, long pulse, four-cavity, high power relativistic klystron amplifier," *Phys. Plasmas*, vol. 26, no. 3, Mar. 2019, Art. no. 033107, doi: 10.1063/1.5086734.
[12] J. Zhang, D. Zhang, Y. Fan, J. He, X. Ge, X. Zhang, J. Ju, and T. Xun, "Progress in narrowband high-power microwave sources," *Phys. Plasmas*, vol. 27, no. 1, Jan. 2020, Art. no. 010501, doi: 10.1063/1.5126271.
[13] Y. Teng, S. Li, D. Wang, X. Wu, D. Yang, X. Li, X. Zhu, W. Tan, and L. Zhang, "Theoretical research on properties of spatial harmonics in corrugated waveguide," *IEEE Access*, vol. 7, pp. 167784–167794, Dec. 2019, doi: 10.1109/ACCESS.2019.2954346.
[14] Y. Teng, D. Wang, S. Li, D. Yang, Y. Shi, P. Wu, and X. Wu, "Theoretical research on power handling capacity of the modes TM_{01} and TM_{02} in corrugated waveguides," *Phys. Plasmas*, vol. 26, no. 5, May 2019, Art. no. 053105, doi: 10.1063/1.5096955.
[15] M. J. Arman, "High-power radial klystron oscillator," *Proc. SPIE*, vol. 2557, pp. 21–31, Sep. 1995, doi: 10.1117/12.218562.
[16] M. J. Arman, "Radial acceletron, a new low-impedance HPM source," *IEEE Trans. Plasma Sci.*, vol. 24, no. 3, pp. 964–969, Jun. 1996, doi: 10.1109/27.533102.
[17] Z. Chen, J. Wang, Y. Wang, G. Wang, S. Li, and G. Cheng, "Novel high-power subterahertz-range radial surface wave oscillator," *Phys. Plasmas*, vol. 22, no. 6, Jun. 2015, Art. no. 063114, doi: 10.1063/1.4923287.
[18] R. L. Wright and E. Schamiloglu, "Experimental evaluation of a radially symmetric transit-time oscillator," in *Proc. Pulsed Power Plasma Sci. 28th IEEE Int. Conf. Plasma Sci. 13th IEEE Int. Pulsed Power Conf. Dig. Papers (PPPS)*, vol. 2, 2001, p. 1614, doi: 10.1109/PPPS.2001.1001874.
[19] Y. Jia, Y. Liu, and Q. Tan, "Primary experimental study on radial transit time oscillator," *High Power Laser Part. Beams*, vol. 15, no. 8, pp. 797–800, Aug. 2003.
[20] F. Dang, X. Zhang, H. Zhong, and Y. Li, "Preliminary experimental investigation of a Ku-band radial line oscillator based on transition radiation effect," *Phys. Plasmas*, vol. 22, no. 9, Sep. 2015, Art. no. 093113, doi: 10.1063/1.4930286.

[21] F. Dang, X. Zhang, J. Zhang, J. Ju, and H. Zhong, "Experimental demonstration of a Ku-band radial-line relativistic klystron oscillator based on transition radiation," *J. Appl. Phys.*, vol. 121, no. 12, Mar. 2017, Art. no. 123305, doi: 10.1063/1.4979309.
[22] F. Dang, X. Zhang, H. Zhong, Y. Li, and Z. Qi, "Simulation investigation of a Ku-band radial line oscillator operating at low guiding magnetic field," *Phys. Plasmas*, vol. 21, no. 6, p. 063307, Feb. 2014, doi: 10.1063/1.4886150.
[23] J. Zhu, X. Zhang, and F. Dang, "A Ka-band radial relativistic backward wave oscillator with GW-class output power," *Phys. Plasmas*, vol. 27, no. 7, Jul. 2016, Art. no. 073111, doi: 10.1063/1.4958316.
[24] S. Li and Z. Yang, "Radial klystron oscillator driven by intense relativistic electron beam," *High Power Laser Part. Beams*, vol. 18, no. 11, pp. 1888–1892, Nov. 2006.
[25] J. F. Zang, Q. X. Liu, Y. C. Lin, and J. Zhu, "Numerical simulation of radial three-cavity transit time oscillator," *High Power Laser Beams*, vol. 20, no. 3, pp. 473–476, Dec. 2008.
[26] J.-C. Ju, L. Liu, and D. Cai, "Characterization of plasma expansion dynamics in a high power diode with a carbon-fiber-aluminum cathode," *Appl. Phys. Lett.*, vol. 104, no. 23, Jun. 2014, Art. no. 234102, doi: 10.1063/1.4882162.
[27] J. He, Y. Cao, J. Zhang, and J. Ling, "Field distributions and beam coupling in the low-impedance transit-time oscillator without foils," *IEEE Trans. Plasma Sci.*, vol. 41, no. 4, pp. 847–852, Apr. 2013, doi: 10.1109/TPS.2012.2233501.
[28] Y. Cao, J. He, J. Zhang, J. Zhang, and Z. Jin, "An oversized *X*-band transit radiation oscillator," *Appl. Phys. Lett.*, vol. 101, no. 17, Oct. 2012, Art. no. 173504, doi: 10.1063/1.4764550.
[29] J. Zhou, D. Liu, C. Liao, and Z. Li, "CHIPIC: An efficient code for electromagnetic PIC modeling and simulation," *IEEE Trans. Plasma Sci.*, vol. 37, no. 10, pp. 2002–2011, Oct. 2009, doi: 10.1109/TPS.2009.2026477.
[30] F. Dang, X. Zhang, and H. Zhong, "Electron motion analysis of a radial-radiated electron beam in a radial-line drift tube with finite magnetic field conducted," *Phys. Plasmas*, vol. 24, no. 2, Feb. 2017, Art. no. 023113, doi: 10.1063/1.4976135.

FANGCHAO DANG was born in Shaanxi, China, in 1988. He received the Ph.D. degree in physical electronics from the National University of Defense Technology (NUDT), Changsha, China, in 2017. He is currently an Associate Researcher with the College of Advanced Interdisciplinary Studies, NUDT. His current research interests include high-power microwave device, intense relativistic electron beam, and microwave radiation systems.

FUXIANG YANG was born in Hunan, China, in 1995. She received the B.S. degree in electromagneticfield and wireless technology from the University of Electronic Science and Technology of China (UESTC), Chengdu, China, in 2017. She is currently pursuing the Ph.D. degree with the College of Advanced Inter-disciplinary Studies, NUDT, Changsha, China. Her current research interest includes vacuum electron devices for high-power microwave generation.

XINGJUN GE was born in Shandong, China, in 1982. He received the Ph.D. degree in physical electronics from the National University of Defense Technology (NUDT), Changsha, China, in 2010. He is currently an Associate Professor with the College of Advanced Interdisciplinary Studies, NUDT. His current research interests include electron beam devices for high-power microwave device, computational techniques in electromagnetics, and pulse power technology.

XINHE WU was born in Shandong, China, in 1988. He received the M.S. degree in physical electronics from the National University of Defense Technology (NUDT), Changsha, China, in 2013. He is currently an Associate Researcher with the College of Advanced Interdisciplinary Studies, NUDT. His current research interests include plasma physics and pulse power technology.

XIAOPING ZHANG was born in Shanxi, China, in 1975. She received the Ph.D. degree in physical electronics from the National University of Defense Technology (NUDT), Changsha, China, in 2004. She is currently a Professor with the College of Advanced Interdisciplinary Studies, NUDT. Her current research interests include electron beam devices for high-power microwave generation, computational techniques in electromagnetics, and pulse power technology.